

1

2 Projections of North American Snow from NA-CORDEX  
3 and their Uncertainties, with a Focus on Model  
4 Resolution.

5 R. R. McCrary<sup>1</sup>, L. O. Mearns<sup>1</sup>, M. Hughes<sup>2</sup>, S. Biner<sup>3</sup>, M. S. Bukovsky<sup>1</sup>

6

7 <sup>1</sup> National Center for Atmospheric Research, P.O. Box 3000, Boulder, CO 80307.

8 <sup>2</sup> NOAA Physical Sciences Laboratory, Boulder, CO, USA

9 <sup>3</sup> Ouranos, Montreal, Quebec

10 \* Corresponding Author: [rmccrary@ucar.edu](mailto:rmccrary@ucar.edu), 1-303-497-2482

11

12 ORCID: <https://orcid.org/0000-0003-0741-6773>

13

14 Resubmitted to Climatic Change on 7 December 2021

15

16 Keywords: climate change, snow, regional climate modeling, North America,  
17 CORDEX

18

19 **Abstract**

20       Snow is important for many physical, social, and economic sectors in North America. In  
21    a warming climate, the characteristics of snow will likely change in fundamental ways, therefore  
22    compelling societal need for future projections of snow. However many stakeholders require  
23    climate change information at finer resolutions than global climate models (GCMs) can  
24    provide. The North American Coordinated Regional Downscaling Experiment (NA-CORDEX)  
25    provides an ensemble of regional climate model (RCMs) simulations at two resolutions (~0.5°  
26    and ~0.25°) designed to help serve the climate impacts and adaptation communities. This is the  
27    first study to examine the differences in end-of-21st-century projections of snow from the NA-  
28    CORDEX RCMs and their driving GCMs.

29       We find the broad patterns of change are similar across RCMs and GCMs: snow cover  
30    retreats, snow mass decreases everywhere except at high latitudes, and the duration of the snow  
31    covered season decreases. Regionally, the spatial details, magnitude, percent, and uncertainty of  
32    future changes varies between the GCM and RCM ensemble, but are similar between the two  
33    resolutions of the RCM ensembles. Increases in winter snow amounts at high latitudes is a  
34    robust response across all ensembles. Percent snow losses are found to be more substantial in the  
35    GCMs than the RCMs over most of North America, especially in regions with high-elevation  
36    topography. Specifically, percent snow losses decrease with increasing elevation as the model  
37    resolution becomes finer.

38

39

40

41 **1. Introduction**

42 Terrestrial snow plays a key role in the climate, ecology, hydrology, and economy of  
43 North America (NA). Snow's high albedo alters the surface energy budget consequently  
44 influencing both long-term climate and short-term weather (e.g. Vavrus, 2007). It also provides  
45 an important habitat for wildlife that are adapted to living in snow conditions (Campbell et al,  
46 2005; Barsugli et al, 2020). Seasonal snow accumulation is a natural reservoir for water storage  
47 and the timing and amount of snowmelt is critical for water supply (Barnett et al, 2005),  
48 agriculture (Qin et al, 2020) and hydropower production (Markoff and Cullen, 2008). The  
49 timing and amount of snowmelt is linked to droughts (Harpold, 2016) and wildfires (Westerling  
50 et al, 2006). Snow is crucial for winter transportation (Palko and Lemmen, 2018) and tourism  
51 (e.g. skiing, snowmobiling, snowshoeing; Chin et al, 2018; Wobus et al, 2017) which drive  
52 regional economies (Burakowski and Magnusson, 2012). In addition to the many benefits of  
53 snow, it also contributes to a wide range of hazards including damages to roads and buildings  
54 (Palko and Lemmen, 2018; Jeong and Sushama, 2018), avalanches (Campbell et al, 2007) and  
55 spring flooding (Berghuijs et al, 2016).

56 Future changes in snow conditions that are expected to be associated climate change will  
57 have important implications for all of these sectors. This drives a strong societal need for  
58 regional projections of snow and their uncertainties. Researchers and stakeholders alike need  
59 such information to determine the regional and local impacts of future changes in snow as well  
60 as to inform decision makers regarding how to adapt to future changes.

61 Changes in snow result from the combined interactions between increasing temperatures  
62 and changing precipitation patterns. Future projections of snow for NA have been investigated  
63 using modeling techniques across multiple time and space scales including global climate models

64 (GCMs; Raisanen, 2008; Brown and Mote, 2009; Mudryk et al, 2020, Krasting et al, 2013),  
65 regional climate models (RCMs; McCrary and Mearns, 2019; Rhoades et al, 2018a; Rasmussen  
66 et al, 2011), variable resolution climate models (Rhoades et al, 2018b), and statistical  
67 downscaling applied to hydrologic models (Christensen and Lettenmaier, 2007; Notaro et al.  
68 2014). These studies show that increasing temperatures will dominate the climate change signal  
69 over most of NA resulting in widespread decreases in snowfall, snow cover extent and duration,  
70 and snow water equivalent (SWE). However, mid-winter snowfall and SWE may increase over  
71 the cold high latitudes and high elevations (Raisanen, 2008; McCrary and Mearns, 2019;  
72 Rasmussen et al., 2011).

73 The North American Coordinated Regional Downscaling Experiment (NA-CORDEX;  
74 Mearns et al, 2017) consists of an ensemble of regional climate projections for NA where  
75 multiple RCMs were driven with boundary conditions from multiple GCMs to produce  
76 downscaled climate projections at two resolutions ( $\sim 0.5^\circ$  and  $\sim 0.25^\circ$ ). NA-CORDEX fills a need  
77 for scientists and stakeholders who desire spatially uniform and consistent climate change data at  
78 higher resolutions than GCMs can provide, and with enough models to explore uncertainty.  
79 RCM ensembles like NA-CORDEX are heavily used across multiple disciplines in order to study  
80 climate change and its impacts (Mearns et al, 2015; McGinnis and Mearns, 2021). While there  
81 exists an abundance of papers examining temperature and precipitation projections in RCM  
82 ensembles, far fewer studies have looked at snow, even over Europe where CORDEX  
83 simulations have been available for longer.

84 Our goal here is to evaluate snow and examine future changes and their uncertainties in  
85 the NA-CORDEX RCMs and their driving GCM simulations. Since NA-CORDEX provides  
86 downscaled simulations at two resolutions, we focus on the differences between the RCM and

87 GCM ensembles to identify what, if any, additional information is gained by increasing  
88 resolution from GCM scales (ranging from  $1.25^{\circ}$  to  $2.8^{\circ}$ ) down to  $0.5^{\circ}$  and  $0.25^{\circ}$ . To do this we  
89 performing a side-by-side comparison of the GCMs and RCMs used in NA-CORDEX, parsing  
90 NA-CORDEX by resolution. We focus on how the spatial distribution, magnitude, and percent  
91 change of future projections and their uncertainties differ across the ensembles. Our analysis  
92 starts broadly over all of NA, but then narrows down to three unique regions (Figure 1a) to  
93 further explore regional differences in model fidelity and future change. In this work, we define  
94 uncertainty as the spread across either the observations or the individual climate model  
95 ensembles.

## 96 **2. Models, Datasets, and Methods**

### 97 **2.1 Models**

98 In NA-CORDEX, multiple RCMs were driven with boundary conditions from multiple  
99 GCMs that were part of phase 5 of the Coupled Model Intercomparison Project (CMIP5; Taylor  
100 et al. 2012). Many of the RCM simulations in NA-CORDEX were performed at two resolutions  
101 ( $0.44^{\circ}$  or 50km and  $0.22^{\circ}$  or 25km, depending on the model configuration). All RCM  
102 simulations cover at least 1951-2098, and future projections (2006-2098) follow the  
103 Representative Concentration Pathway 8.5 (RCP 8.5). In this work the historical time period  
104 spans 1976-2005 and the end-of-21st-century future time period spans 2070-2098.

105 We analyze the subset of NA-CORDEX simulations that have SWE output (Table 1).  
106 Although SWE is available from the RegCM4 NA-CORDEX simulations ([na-cordex.org](http://na-cordex.org)),  
107 unbounded snow accumulation was found to occur in many mountainous regions so this RCM  
108 was excluded from the analysis (Supplemental Information (SI) Section S1). We split the NA-  
109 CORDEX models into two climate ensembles based on resolution. As discussed more in Section

110 2.3.2, we regrid the  $0.44^\circ/50\text{km}$  simulations to a common  $0.5^\circ$  grid, and the  $0.22^\circ/25\text{km}$   
111 simulations to a common  $0.25^\circ$  grid. Throughout the paper we refer to these ensembles as either  
112 NA-CORDEX- $0.5^\circ$  (8 members) or NA-CORDEX- $0.25^\circ$  (11 members).

113 Of the 7 driving GCMs used in NA-CORDEX, daily SWE was available from 6 (Table  
114 1). Throughout the paper we refer to this set of 6 GCMs as the CMIP5-Driver ensemble. We  
115 also look at broad changes in SWE from all of the models in CMIP5 with daily SWE output  
116 which we refer to as the CMIP5-ALL ensemble (SI Table S1, 18 members). In our analysis, the  
117 CMIP5-All ensemble is included on all timeseries plots, but not on the spatial maps.

118 **2.2 Snow Datasets**

119 A major challenge for evaluating SWE in climate models is a lack of long-term, high-  
120 resolution (spatial and temporal), well-vetted gridded observations (e.g. McCrary et al,  
121 2017). The insufficiency of snow observations has led many to create gridded SWE datasets that  
122 are observationally-constrained and informed by models, which we call Modeled-Observations,  
123 or MObservations (MObs). These include atmospheric and land-surface reanalysis products and  
124 statistical and physical models that are constrained by in-situ snow observations.

125 Following McCrary et al, (2017) we use a multi-dataset approach to capture the  
126 uncertainty in observed snow by creating an ensemble of MObs datasets (Table 2). All of the  
127 MObs datasets included are gridded products with  $0.25^\circ$  or finer resolution, at least 5 years of  
128 data between 1981-2010, and cover CONUS or North America. These datasets have considerable  
129 uncertainties related to sparse observational networks and surface meteorological forcing,  
130 satellite retrieval algorithms, and the use of models that must parameterize snow processes.  
131 While this ensemble will not capture the full uncertainty in snow observations, it serves as a  
132 reference dataset in which to assess the climate models used in this study.

133           Optical satellite products can be used to identify the presence of snow. To evaluate snow  
134    cover metrics we include the Interactive Multisensor Snow and Ice Mapping System (IMS)  
135    24km daily snow cover dataset (U.S. National Ice Center, 2008) in combination with snow cover  
136    estimated from the SWE MObs.

137    **2.3 Methods**

138    *2.3.1 Calculation of Snow Cover*

139           Similar to McCrary and Mearns (2019), we calculate snow cover from SWE by applying  
140    a 5mm threshold to daily SWE fields from the MObs and the simulations to produce a binary  
141    yes-no snow cover field. Snow cover extent (SCE) is calculated by first averaging this binary  
142    field over each month to produce monthly snow cover fraction (SCF) at each gridbox and then  
143    summing over NA. The daily binary snow cover field is also used to calculate snow cover  
144    duration (SCD), defined as the number of days with snow on the ground. SCE, SCF and SCD  
145    are also calculated from the satellite IMS dataset which provides estimates of yes-no snow cover.  
146    Snow-on-ice (sea ice or land ice) is a complex process that is not well simulated by many climate  
147    models. We remove any points which may be ice covered or strongly influenced by land/sea ice.  
148    See SI Section S3 for a description of how these points were removed.

149    *2.3.2 Ensemble Analysis*

150           As regridding snow onto different grids can greatly impact mass budgets, regionally  
151    averaged time series plots are calculated on the native grids of the climate models. However,  
152    since each model uses a different grid, for ensemble mean spatial calculations we regridded the  
153    MObs and models to common grids using conservative remapping. The CMIP5 models have

154 been regredded to a  $1.5^{\circ}$  grid, and the NA-CORDEX ensembles have been regredded to  $0.5^{\circ}$  and  
155  $0.25^{\circ}$ .

## 156 **3. Results**

### 157 **3.1 Evaluation of Climate Models**

158 In the following section we compare the historical simulations from the CMIP5 and NA-  
159 CORDEX ensembles with the MObs ensemble.

#### 160 *3.1.1 Snow Cover Extent*

161 The annual cycle of SCE from the MObs and climate models is shown in Fig 2. Only,  
162 IMS and ERA5-land have daily data covering all of NA. The timing of the annual cycle of SCE  
163 in the MObs follow each other closely. SCE is near zero in July-August, starts to increase in  
164 September, reaches a maximum in January and declines throughout the spring and early summer.  
165 Between December-April IMS has higher values than ERA5-land, otherwise the two datasets are  
166 closely matched the rest of the year. Spatially, the largest differences in January snow cover  
167 fraction (SCF) occur in the Central Plains and Great Basin (SI Fig. S4.)

168 Ensemble mean SCE for the CMIP5-Driver and CMIP5-All ensembles are similar to each  
169 other and are lower than both MObs (Fig. 2; individual models results SI Fig. S8). The spread in  
170 historic SCE in the both CMIP5 ensembles is much larger than the MObs spread. In both NA-  
171 CORDEX ensembles, the ensemble mean annual cycle of SCE is on the higher end of the MObs,  
172 following the IMS dataset almost exactly, with half the individual RCMs slightly overestimating  
173 SCE compared to IMS (SI Fig. S8). The spread in the NA-CORDEX- $0.5^{\circ}$  ensemble is larger  
174 than the NA-CORDEX- $0.25^{\circ}$  ensemble, primarily due to the HIRHAM5 EC-EARTH simulation  
175 being a low outlier which is only present in the  $0.5^{\circ}$  ensemble (SI Fig S8). The spatial

176 distribution of January snow cover fraction (SCF) highlights where differences in simulated SCE  
177 arise (SI Fig. S5-S7).

178 *3.1.2 Climatological SWE*

179 Maps of ensemble mean annual maximum monthly SWE (AM-SWE) from the MObs and  
180 climate simulations are shown in Fig. 3. For the MObs, ensemble mean AM-SWE is calculated  
181 across all available datasets at each gridbox (Fig 3a-c). Although the spatial patterns of AM-  
182 SWE are similar across the three resolutions, distinct topographic features such as the Sierra  
183 Nevada's in California, the Cascade Range in the Pacific Northwest, and the Rocky Mountains  
184 deteriorate with decreasing spatial resolution. Results from the individual MObs and MObs  
185 ensemble statistics highlight the uncertainty across the MObs ensemble (SI Figs. S9-S12). In  
186 this study we use them as a reference to qualitatively evaluate the models.

187 The spatial patterns of AM-SWE in the CMIP5-Driver and NA-CORDEX ensembles are  
188 broadly similar to the MObs ensemble (Fig 3 d-f; individual model results SI Figs. S13-  
189 15). Compared to the MObs ensemble mean, the CMIP5-Driver GCMs underestimate SWE in  
190 the mountains and overestimate SWE in the lower elevation regions of western NA (Fig. 3. d,g,j;  
191 SI Fig. S16). As the mountains in these coarse GCMs are relatively smooth and low (Fig. 1b)  
192 there is limited orographic enhancement of precipitation in the mountains resulting in too much  
193 moisture penetrating inland, likely contributing to positive biases east of the mountain ranges in  
194 the west (e.g., Rasmussen et al, 2011). The smoothed topography in the GCMs also results in  
195 artificially high terrain in the interior valleys of western NA, which likely contributes to cold  
196 biases, and excess SWE accumulation and suppressed ablation. In the CMIP5-Driver ensemble  
197 negative biases also occur over most of Canada. AM-SWE in the CMIP5-Driver ensemble falls

198 within the range of the MObs over much of CONUS, however biases fall outside the MOBs  
199 range near the western mountains and Northeast Canada (SI Fig. S19) .

200 AM-SWE in the two NA-CORDEX ensembles differs from the MObs ensemble in  
201 similar ways (Fig 3, h,i,k,l; individual model results SI Figs. S14-S15, S17-S18). The only real  
202 difference is that the spatial details of SWE patterns are finer with increasing resolution. In both  
203 ensembles, positive biases dominate over the domain, with negative biases near some mountains  
204 and across central Canada. Over the western half of the domain, AM-SWE is greatly  
205 overestimated on the western side of the mountains and underestimated just east of the highest  
206 peaks of the mountains (SI Fig. S20). Relative to the MObs ensemble mean, the magnitude of  
207 positive SWE biases are larger in the mountains than the lower elevation regions, however,  
208 percent SWE biases are much larger at lower altitudes. The percent bias figures (Fig. 3 j-l)  
209 highlight regions where the climate models simulate snow but the MObs do not. When  
210 compared to the range of the MObs ensemble, AM-SWE values in both RCM ensembles are  
211 greater than the MObs on the western side of Mountain ranges, in the Central US, and Northern  
212 Canada/Alaska (SI Fig. 19).

213 The similarities in the AM-SWE bias patterns in the RCMs suggests that biases in large-  
214 scale forcing and RCM configuration/parameterizations play a similar role in the simulation of  
215 SWE at both resolutions. As the mountains in the NA-CORDEX simulations are higher than the  
216 GCMs, orographic precipitation is larger in the RCMs due to enhanced lifting (See Mahoney et  
217 al, 2021) resulting in higher SWE values. However, winter precipitation in NA-CORDEX far  
218 exceeds observations in the RCMs (Mahoney et al, 2021). This is possibly because even at 0.25°  
219 convection is insufficiently resolved and convective parameterizations play a large role in  
220 precipitation biases (Hughes et al. 2021). The bias in precipitation likely translates to a positive

221 bias in SWE, however SWE biases will also be linked to temperatures the evolution of snowpack  
222 in the RCMs (McCrary et al., 2017).

### 223 *3.1.3 Snow Cover Duration*

224 The length of the snow covered season or SCD may also change in the future. In the  
225 MObs, SCD increases with latitude and elevation (Fig. 4a-f; individual MObs in SI Figs. S21-  
226 S23). The broad spatial patterns of SCD are similar across the different resolutions, but the  
227 details are lost as resolution coarsens. Much like winter SWE values, SCD is reduced in the  
228 mountains when aggregated to coarse scales (Fig. 4a).

229 The CMIP5-Driver GCMs underestimate SCD in the mountains and most of the eastern  
230 half of the domain, although SCD is positively biased at low-elevation regions in the western  
231 half of the domain (Fig. 4g; individual models results SI Fig S24). Both RCMs ensembles  
232 overestimate SCD over most of the domain, with larger positive biases at lower-elevation in the  
233 Great Basin and east of the middle and southern Rockies and negative biases over north-central  
234 Canada (Fig. 4h,i; individual model results SI Figs. S25-S26 ).

## 235 **3.2 Future Change over North America**

### 236 *3.2.1 Snow Cover Extent*

237 SCE is projected to decrease in all months of the year in all of the models examined (Fig.  
238 2, c-d; individual model results SI Fig. S8). The largest percent losses are projected to occur in  
239 October, May and June when snow cover is marginal in the historic climate period. Average  
240 SCE losses are larger in both CMIP5 ensembles than both NA-CORDEX ensembles. Although  
241 ensemble mean changes in SCE are similar for the CMIP5-Driver and CMIP5-All model  
242 ensembles, the uncertainty (measured here as the multi-model spread) is considerably larger in

243 the CMIP5-All ensemble. This may indicate that our subset of CMIP5 models does not capture  
244 the full potential of the combination of temperature and precipitation changes that drive changes  
245 in snow. The NA-CORDEX 0.5° and 0.25° ensembles have nearly identical projections for SCE  
246 loss, both of which are smaller than the CMIP5-Driver ensemble mean. The uncertainty in  
247 future SCE changes is slightly larger in the NA-CORDEX ensembles than the CMIP5-Driver  
248 ensemble during October-February but slightly smaller in March-July.

249 *3.2.2 Annual Maximum SWE*

250 All three model ensembles project large-scale losses in AM-SWE over most of the  
251 domain, with the exception of the high-latitude regions of NA (Fig. 5; individual model results  
252 SI Figs. S27-S32). These results are consistent with previous studies (McCrary and Mearns,  
253 2019; Raisanen, 2008). Absolute losses are larger in the mountains over the western and eastern  
254 portions of the domain, while percent losses are higher at low latitudes and lower  
255 elevations. Total snow losses are projected in all of the ensembles along the southern edge of the  
256 snow boundary (Fig 5. d-f). The individual models in all of the ensembles also show total losses  
257 along the southern snow boundary (SI Figs. S28, S30, S32).

258 While the three ensembles tell broadly the same story, details emerge in the RCMs, that  
259 are not found in the GCMs. Focusing on percent change, as it reduces the influence of simulated  
260 difference in baseline historical AM-SWE amounts, it is apparent that percent losses are  
261 generally larger in the CMIP5-Driver ensemble than in both of the NA-CORDEX RCM  
262 ensembles, especially in regions of complex topography. By the end of the 21<sup>st</sup> century, the  
263 CMIP5-Driver ensemble projects that 50.5% of NA will experience AM-SWE losses of greater  
264 than 50% and that 15.9% of NA will experience losses of greater than 90%. While the NA-  
265 CORDEX-0.5° ensemble projects greater than 50% losses over 38.9% of NA and 90% losses

266 over 9.16% of the domain, the NA-CORDEX-0.25° ensemble projects greater than 50% losses  
267 36.4% of NA and 90% losses over 8.8%. The reduced losses in the RCMs is partially due to the  
268 fact that they have more higher-elevation mountain points (Fig. 1 and Section 3.1.1) where  
269 temperatures can remain below freezing during winter. But also, percent change is affected by  
270 the historical snow amount where for the same magnitude loss, smaller percentage loss will be  
271 found if there is more SWE in the historical baseline climate.

### 272 *3.2.3 Snow Cover Duration*

273 Along with losses in SCE and SWE, the duration of the snow covered season is also  
274 projected to decrease (Fig. 4, j-l; individual model results SI Figs S33-S35). The largest  
275 decreases in SCD are found over the mountains in the western half of the domain, over  
276 Southwestern Alaska, and the eastern half of Newfoundland/Labrador and New England. While  
277 the broad spatial patterns of changes in SCD are similar across the ensembles, again the spatial  
278 details are lost in the GCMs. For example, in the western mountains the RCMs demonstrate that  
279 SCD will decrease more at higher elevations than lower elevations. While AM-SWE is  
280 projected to increase at high-latitudes (Fig 5) and at high-elevations in a few of the models (SI  
281 Figs. S28, S30, S32), SCD is found to decrease everywhere, indicating while AM-SWE may  
282 increase in some locations, the snow covered season will still contract.

## 283 **3.3 Regional Changes**

284 In the previous section we explored the continental-scale patterns of changes in snow  
285 conditions over NA. While important from a large-scale climate perspective, most researchers  
286 and stakeholders often want to know what will happen over smaller-scale regions. Here we  
287 zoom in on three unique climate regions, to explore more deeply how resolution influences  
288 future projections of SWE. These regions (Fig. 1a) are, the U.S. Intermountain West (IMW),

289 North-Central Canada (NC-Canada), and Northeast U.S. and Southeast Canada (referred here as  
290 the Northeast). The considerable changes in snow projected along the west-coast of the domain  
291 in the NA-CORDEX models have been explored in Rhoades et al. (2018a) and Mahoney et al.  
292 (2021).

293 *3.3.1 U.S. Intermountain West (IMW)*

294 The IMW region is large and contains portions of the middle and southern Rocky  
295 Mountains and the Great Basin (Fig. 1a). We chose this region because of its complex  
296 topography including high elevation mountains where seasonal snowpacks and spring snowmelt  
297 are critical for water supply, ecosystem health, forest fire risk, and recreation.

298 First we examine the annual cycle of monthly averaged total snow mass (SM) for the  
299 region (Fig. 6 a,d; individual models results SI Fig. S36). The observational uncertainty is very  
300 high as the MObs disagree on the magnitude of SM during most months of the year (excluding  
301 August and September) and the timing of peak SM (showing either a February or March  
302 maximum). There is a clear separation between the 4 highest MObs and the 3 lowest MObs over  
303 the region. Lundquist et al. (2020) demonstrated that most snow reanalysis datasets  
304 underestimate SWE in the mountains, so our judgement here is that datasets with higher SM  
305 values are more realistic.

306 The spread in historical SM in both CMIP5 ensembles is larger than the spread of the  
307 MObs with a few GCMs greatly underestimating peak SM. Ensemble mean SM in the GCMs  
308 falls within the middle of the MObs range. The NA-CORDEX ensembles have considerably  
309 more snow than their driving GCMs and about half the spread during peak months. Between  
310 December-April, ensemble mean SM in the RCMs falls within the 4 highest MObs, but spring  
311 snowmelt occurs more rapidly in the RCMs than those same datasets.

312 To examine future changes in regional SM, we again primarily focus on percent changes  
313 (Figure 6 h,k), however, the annual cycle of future snow and the magnitude of snow changes are  
314 shown in SI Fig. S37. Average IMW SM is projected to decrease for all months of the year in all  
315 of the models, except for one CMIP5-ALL ensemble member (Fig. 6, h,k). Regional percent SM  
316 losses are smaller in the NA-CORDEX ensembles than the CMIP5 ensembles. For example, in  
317 March (around the timing of peak snow amounts) SM is projected to decrease by 84.1% in  
318 CMIP5-ALL, 76.8 in CMIP5-Driver, 58.2% in NA-CORDEX-0.5°, and 52.4% in NA-  
319 CORDEX-0.25°. The uncertainty in future losses is also much larger in the GCM ensembles  
320 than the RCM ensembles. For example, in March the spread in future change is 2.05 times larger  
321 in the CMIP5-ALL ensemble than the NA-CORDEX-0.25° ensemble. In most of the models the  
322 largest absolute SM losses occur when historical maximum SM occurs, and the timing of peak  
323 SM occurs one month earlier in the future (SI Fig. S36-S37).

324 Fig. 7 examines the spatial distribution of historical and future changes in AM-SWE  
325 over the IMW. Terrain plays a large role in determining precipitation, snowfall and SWE  
326 patterns in the IMW. In the coarse CMIP5-Driver GCMs, topography is fairly smooth and the  
327 Rocky Mountains are captured as one mountain feature (Fig 7a) although this varies slightly with  
328 GCM, see SI Fig. S38). With increasing resolution, individual mountain ranges begin to appear  
329 and become more distinct (Fig 7b-c). Comparisons of the distribution of elevation over the IMW  
330 (Fig. 8a) highlights that all of the ensembles, but in particular the CMIP5-Driver ensemble, have  
331 too many grid points at mid-elevations between 1500-2500m and too few points at lower  
332 elevation valleys and higher elevation mountains.

333 In both the historical and future simulations, AM-SWE generally increases with elevation  
334 and latitude (Fig 7d-i; individual models SI Figs. S39-S41). As with topography, distinct spatial

335 patterns of SWE become more refined with increasing resolution. Comparison to the MObs  
336 AM-SWE (SI Fig. 20) reveals unrealistic patterns in the CMIP5-Driver ensemble related to the  
337 GCMs' unrealistic underlying terrain, as the Middle and Southern Rockies should have distinct  
338 peaks in SWE.

339 By the end of the century, ensemble mean AM-SWE is projected to decrease at all  
340 gridpoints over the IMW region in all of the ensembles, (Fig. 7 g-i) although some individual  
341 models do have regions with small increases (SI Figs. S42-S47). In terms of magnitude, the  
342 largest losses generally correspond with the largest historical SWE values (in the high elevations  
343 and northern part of the domain) (Fig. 7j-l; individual model results SI Figs S42-S44). However,  
344 the largest percent losses can be found at lower elevation, lower latitude regions, with smaller  
345 percent losses projected at high elevations (Fig. 7m-o; individual model results SI Figs S45-S47).  
346 The RCM ensembles both have lower percent losses than the GCMs in many areas, which appear  
347 for the most part to correspond with higher topography. Although temperatures are projected to  
348 increase everywhere over the IMW, we might expect higher-elevation SWE to be partially  
349 preserved as temperatures can still remain below freezing during the heart of winter.

350 To further explore the relationship between elevation and snow over the IMW we bin  
351 annual maximum snow mass (AM-SM) over the IMW by elevation (Fig. 8). To calculate AM-  
352 SM we take the climatological AM-SWE (e.g. Fig 7) from each model and the four highest  
353 MObs in Fig. 6a and calculate the mass of snow stored in each elevation bin for each dataset.

354 None of the datasets have grid points below 500m, the CMIP5-Driver models have no  
355 grid-points above 3000m, and only the MObs and the NA-CORDEX-0.25° ensemble have grid-  
356 points above 3500m (Fig. 8a). Most of the observed AM-SM occurs between 2000-3000m (Fig.  
357 8b), with lower values at higher and lower elevations. In the climate models, most of the AM-

358 SM occurs at lower elevations, between 1500-2500m. On average the RCMs overestimate AM-  
359 SM at mid elevations (1500-2500m) and underestimate AM-SM above 2500m, with larger biases  
360 in the NA-CORDEX-0.5° ensemble. The GCMs skew toward negative AM-SM biases, except  
361 between 1500-2000m, where ensemble mean values are slightly higher than observed. There is  
362 also large uncertainty in historical AM-SM in the CMIP5-Driver ensemble between 1500-  
363 2500m, likely linked with the large spread horizontal resolution and topography (SI Fig S38 and  
364 Fig 8a).

365 In terms of magnitude, the largest losses in AM-SM for all the models occurs between  
366 1500-2500m, corresponding with the elevations bins with the largest historical AM-SM. Percent  
367 losses in the CMIP5-Driver GCMs are also highest between 1500-2500m, but in the RCMs,  
368 percent losses are highest at lower elevations (1000-2000m). In all the models, percent losses  
369 steadily decrease above 2000m, where temperatures will remain below freezing more frequently  
370 than the lower elevation bins. Since vast majority of gridpoints in the GCMs occur between  
371 1500-2500m where the largest AM-SM losses (magnitude and percent) occur and the GCMs  
372 have no gridpoints at the higher elevation bins, this supports the idea that reduced relative snow  
373 losses occur in the RCMs because they have higher mountain elevations, which help to buffer  
374 snow losses. However, percent AM-SM losses are higher in the GCMs at all elevation bins,  
375 which suggests differences are not solely due to elevation, but also related to baseline SM  
376 amounts (Fig. 8b) and the magnitude of total SM loss that occurs in each elevation bin (Fig. 8c)

### 377 *3.3.3 North-Central Canada (NC-Canada)*

378 We next examine changes over North-Central Canada (NC-Canada, Fig. 9) as this is the  
379 one area of NA where the climate model ensembles project potential increases in winter  
380 snowpacks. In this region, increases in SWE could have important implications for winter

381 transportation, wildlife, and indigenous populations. Here we examine how robust these  
382 projected changes are.

383 Only three members of MObs ensemble have SWE data for NC-Canada, and there are  
384 large difference between them (Fig 6b,e; individual model results SI Fig. S48). Also, given the  
385 very few in-situ observations (snow or surface meteorology) over the region (e.g. Mekis et al,  
386 2018), observed snow amounts are highly uncertain. Over NC-Canada, much of the year is snow  
387 covered, with only a short snow-free period in summer. Snow accumulates between October and  
388 March/April and declines quickly between March/April and July, with the timing of peak SM  
389 varying across the datasets. Over the region, ERA5-land has the highest SM values compared to  
390 CMC and GlobSnow. Values are likely underestimated in GlobSnow, as the mountains in the  
391 south-west part of the domain are masked (see SI Fig. S11). SM in all four of the model  
392 ensembles lie on the upper-end of the MObs estimates (following ERA5-land). The spread is  
393 higher in the GCM simulations than the RCM simulations and the RCMs tend to have more  
394 snow than the GCMs.

395 In the future, losses are projected in all of the models examined between May-  
396 November. However, from December-April most of the RCMs and many of the GCMs project  
397 up to 20% increases in SM for the region. Snow increases in this region are likely associated  
398 with increases in the amount of moisture in the atmosphere associated with warming  
399 temperatures which result in increases in precipitation and snowfall, as winter temperatures  
400 remain well below freezing (Raisanen, 2008). In the future the timing of peak SM occurs one  
401 month earlier in most of the models, and the largest magnitude decreases in SM occur in May for  
402 all ensembles (SI Figs. S48-S49).

403            Spatially, most of the increases in AM-SWE occur over the northern and eastern portions  
404    of the domain (Fig. 9) although this is model dependent (SI Figs. S50-S58). At individual points,  
405    ensemble mean AM-SWE increases by 1-50mm or 1-20%. The areal extent over which AM-  
406    SWE is projected to increase is largest in the NA-CORDEX-0.5° ensemble, and smallest in the  
407    CMIP5-DRIVER ensemble. All of the models in all of the ensembles project increase in SWE  
408    along the northern edge of continental Nanavut (Fig. 9, p-r); however, model agreement  
409    regarding where increases in SWE may occur is lower for the west and south of the domain.

410    *3.3.3 Northeast U.S. and Southeast Canada (Northeast)*

411            While the vast majority of previous studies have examined future projections for snow  
412    over western NA, snow is also important over the Northeast (Fig. 1a). In this region, heavy  
413    snowfall and snow loads are hazards for transportation and building infrastructures and snowmelt  
414    plays a key role in spring flooding. The Northeast region is also home to over 180 ski resorts  
415    (<https://www.skicentral.com/>). Lake effect snow may play a role in driving SWE amounts in this  
416    region, and the ability of the models to capture lake effect snow will depend on if the models use  
417    a lake model for the Great Lakes or interpolate lake temperatures from sea surface temperatures  
418    (see RCM Characteristics at <https://na-cordex.org/>).

419            As in the previously examined regions, the spread across the MObs ensemble is  
420    substantial over the Northeast (Fig. 6c). There is also disagreement on whether SM peaks in  
421    February or March over the region. Compared to the MObs the spread in both the CMIP5  
422    ensembles is larger than the estimated observed spread, with the ensemble mean values falling in  
423    the middle of the MObs (Fig. 6c, SI Figs. S59-S60). The spread across the NA-CORDEX RCMs  
424    is smaller than the MObs, with the RCMs following the upper end of the MObs (Fig. 6f). It is  
425    possible that all of the MObs underestimate SWE in the region, as observations are limited.

426 Substantial losses are projected for the region in all of the models (Fig. 6 j-m; individual  
427 model results SI Figs. S59-S60). Percent losses are largest October-November and April-May,  
428 and smaller in the middle of winter. However, even in winter, most models project that the  
429 region will lose more than 40% of its total SM. The uncertainty range for SM losses is twice as  
430 large in the CMIP5-All ensemble than the CMIP5-Driver ensemble, again suggesting CMIP5-  
431 Driver models may not capture the full range of climate possibilities. Regional scale losses are  
432 nearly identical in the two NA-CORDEX ensembles. The uncertainty of the change in the  
433 RCMs is smaller than the CMIP5-All ensemble, but larger than the CMIP5-Driver ensemble.

434 At first glance, the spatial representation of winter SWE in the CMIP5-Driver and NA-  
435 CORDEX RCM ensembles appears to be very similar, with higher values in the Northeast  
436 portion of the region, and lower values to the Southwest (Fig. 10, d-f; SI Figs. 61-69). However,  
437 an examination of the spatial details and comparison with topography highlights that even  
438 though topographic variations are less extreme in this region than in the IMW, mountains still  
439 play a role in driving SWE patterns (e.g. Adirondack Mountains in New York).

440 The broad spatial patterns of SWE changes for the end of the century are similar across  
441 the ensembles, with larger total losses to the northeast and smaller total losses to the south and  
442 larger percent losses over the southern portion of the domain and smaller relative losses over the  
443 north. However at closer inspection we see that percent snow losses are smaller with increasing  
444 elevation and higher resolution, indicating topography also dampens snow losses here. While  
445 beyond the scope of this study past RCM studies suggest warming of the Great Lakes may result  
446 in increased lake-effect snowfall possibly mitigating some snow losses in the future (e.g. Notaro  
447 et al, 2015).

448 **4. Summary and Discussion**

449 RCM ensembles like NA-CORDEX are widely used by scientists and stakeholders across  
450 multiple fields. While a plethora of studies have examined temperature and precipitation  
451 changes, far fewer have examined critical variables such as snow. In this study we performed a  
452 side-by-side comparison of historical and future snow over NA between the NA-CORDEX  
453 dynamically downscaled  $0.5^{\circ}$  and  $0.25^{\circ}$  RCM simulations and their driving GCMs ( $1.25^{\circ}$ - $2.8^{\circ}$ ).  
454 The primary goals of this study were to evaluate model performance and examine how end-of-  
455 century projections for snow differ between the different resolution ensembles.

456 To evaluate model performance, we used an ensemble of observationally constrained  
457 SWE datasets. We demonstrate that the uncertainty in gridded snow datasets is large, even  
458 across datasets with high resolutions. This uncertainty is associated with difficulties in  
459 measuring snow and is a major challenge for the snow science community.

460 In their historical climate simulations, the CMIP5-Driver and CMIP5-ALL ensembles  
461 underestimate NA while both NA-CORDEX ensembles tend to follow the higher end of the  
462 MObs. Simulated biases in SCE can have an impact on the radiation budget thereby influencing  
463 surface temperatures and weather patterns (Vavrus et al, 2007 ). On average the CMIP5-Driver  
464 ensemble underestimates AM-SWE and SCD over eastern Canada and at high elevations, but  
465 overestimate them everywhere else. In both RCM ensembles, AM-SWE and SCD biases are  
466 positive everywhere except the highest elevations and across tracts of central Canada. While the  
467  $0.25^{\circ}$  simulations have greater spatial details and higher mountains than the  $0.5^{\circ}$  models, the  
468 spatial pattern of SWE and the magnitude of the biases are similar between the ensembles. Over  
469 the three regions examined, the spread in historical SM is greater across the GCM ensembles  
470 than the RCM ensembles, especially in the IMW and Northeast regions.

471        End-of-century projections for snow over NA are broadly similar across the ensembles  
472    considered. In all ensembles, SCE, AM-SWE, and SCD are projected to decrease over most of  
473    NA, with the exception of increases in AM-SWE at high-latitudes. In terms of magnitude, the  
474    largest losses in AM-SWE and SCD occur over the mountains in the western half of the domain  
475    and over coastal-eastern Canada. However, percent losses in AM-SWE are largest at low-  
476    elevations and low-latitude regions. Comparison of these ensembles shows that in terms of  
477    percent change, which can be more useful in the application of climate model data to climate  
478    change impacts, the CMIP5 GCMs tend to project a more severe picture of total snow loss for  
479    NA. For example, the CMIP5-Driver ensemble project that just over half of NA will experience  
480    greater than 50% losses in AM-SWE, while the RCMs that only 36-38% of NA will experience  
481    greater than 50% losses in AM-SWE. These differences are likely largely related to the poor  
482    representation of topography in the GCMs, but are also related to differences in baseline snow  
483    amounts (see more below).

484        While the large-scale picture of future changes in snow are similar between the  
485    ensembles, zooming in on individual regions helps highlight where differences between the  
486    ensembles occur. Over the IMW and Northeast regions, percent SM losses are larger in the  
487    GCMs than the RCMs, while over NC-Canada percent increases in winter SM are smaller in the  
488    GCMs. The uncertainty in these future changes is larger in the CMIP5-Driver GCMs than the  
489    RCM ensembles over the IMW and NC-Canada, but smaller in the Northeast region. While SM  
490    is projected to decrease during all months of the year in all of the models over the IMW and  
491    Northeast region, 70% of the models examined show winter SM increasing over NC-Canada.  
492    The largest differences across the ensembles are found over the IMW region where topography  
493    plays a large role driving snowfall and SWE amounts through orographic enhancement of

494 precipitation and lower temperatures. As the GCMs oversample low-to-middle elevations and  
495 under-sample the higher elevations, historical SM is under-represented at most elevations,  
496 percent snow losses are larger in the GCMs than the RCMs at most elevations, and the GCMs  
497 have no information about snow at the higher elevations. Our results suggest that a that a more  
498 accurate representation of snow (especially at high elevations) allows for the buffering of snow  
499 losses, which we don't see in coarse models. In contrast to the IMW, over NC-Canada the GCM  
500 and RCM ensembles also show the greatest agreement in historical SM and percent SM changes  
501 in this region, which we suspect could be due to the lack of significant topographic features in  
502 the region.

503 Overall, while we find interesting differences in the specific regional details between the  
504 between the CMIP5-Driver GCMs and the NA-CORDEX RCMs, we do not see significant  
505 differences between two NA-CORDEX ensembles. The largest differences between the GCMs  
506 and RCMs are found in regions of complex topography, but even over the IMW the two RCM  
507 ensembles have very similar climate change responses. So while the spatial details of snow are  
508 more refined in the  $0.25^{\circ}$  ensemble, the overall impact to regional snow is small. However, as  
509 shown in Walton et al (2021), fine-scale details associated with snow in the mountainous may be  
510 important for end-users who statistically downscale temperature from climate models, as  
511 incorrectly capturing snow to no-snow transitions in the future can result in the incorrect  
512 amplification of surface temperatures associated with the snow albedo feedback.

513 While these results are similar to other studies which have examined snow over NA (e.g.  
514 McCrary and Mearns, 2019; Rasmussen et al. 2011). Our study highlights that the severity of  
515 future changes in snow, their uncertainties, and regional details are a function of the size and  
516 configuration of the model simulations/ensembles examined and the resolution of the

517 simulations. The result that the GCMs tend to project a more severe picture of relative snow  
518 losses, in part because they have fewer high-elevation points, is important to remember when  
519 considering studies such as Diffenbaugh et al (2012), which used the CMIP5 models to assess  
520 hydrologic extremes and water availability over regions of the Northern Hemisphere, including  
521 the western US.

522 There are also a few notable limitations to this study. First, while our focus has been on  
523 how increases in resolution impacts the representation of historical and future snow over NA and  
524 their uncertainties, the NA-CORDEX-0.5° and NA-CORDEX-0.25° ensembles consist of  
525 different combinations of RCM/GCM pairs. These differences in ensemble configuration may  
526 also contribute to the differences we found in this study. As discussed in McGinnis and Mearns  
527 (2021), funding was extremely limited for NA-CORDEX and the choice of simulations included  
528 in the experiment was opportunistic and required leveraging other modeling activities (McGinnis  
529 and Mearns, 2021). While the archive consists of simulations with available SWE from 5 RCMs  
530 driven with boundary conditions from 7 GCMs with simulations performed at 2 resolutions  
531 (Table 2), the simulation matrix itself is both sparse and unbalanced, limiting our ability to dive  
532 deeply into the different roles the choice of RCM, GCM, or resolution have on climate change  
533 uncertainty. In this work we chose to include all available ensemble members to highlight the  
534 differences in the available datasets that end users may consider. In SI Section S17, we compare  
535 results from using the full ensemble with the 7 simulations that have matching RCM/GCM pairs  
536 and both resolutions. We find the uncertainty in the historical simulations to be lower in the  
537 smaller subset of models, but that the projections of future change and their uncertainties for all  
538 snow variables are similar between the full and subset ensembles.

539           Second, while the NA-CORDEX simulations are higher resolution than their GCM  
540           counterparts, they are still relatively coarse for capturing precipitation, snowfall, and SWE  
541           especially in topographically complex areas. Many of the sectors discussed in the introduction  
542           require very high resolution data to study the impacts of future changes in snow. Statistical  
543           downscaling techniques are often employed to get at very high-resolution climate information,  
544           but this can break the coupling between the atmosphere and the land-surface leading to  
545           inconsistent results especially in snow dominated regions (Walton et al, 2021).

546           Past RCM studies have found that resolutions of 4-6km to be necessary to match in-situ  
547           point observations of precipitation, snowfall, and SWE (Garvert et al, 2007; Rasmussen et al,  
548           2011). The argument for this is that terrain-induced convection and local air circulation patterns  
549           associated with smaller ridges and valleys that are important for snowfall patterns are better  
550           resolved, and surface temperatures are better represented. Wind redistribution of snow is also  
551           important, which is also not captured in many models (Musselman et al, 2015). Many high-  
552           resolution modeling studies have examined changes in snow over regions of NA (e.g. Sun et al,  
553           2019; Rasmussen et al, 2011; Musselman et al, 2017). While these studies have been able to  
554           look at detailed process level changes that are important, they have been limited in either domain  
555           size or by the use of only one RCM or one GCM, limiting the examination of uncertainty. As  
556           computing power, storage, and analysis of big data continues to advance, we expect to see the  
557           creation of larger ensemble convection permitting simulations (CPSs) over larger domains. The  
558           coordination of regional CPSs is ongoing over Europe in one CORDEX Flagship Pilot Study  
559           (Coppola et al, 2020), but such studies are not being coordinated over NA yet. Until that time,  
560           NA-CORDEX fills a need in the community as it provides spatially uniform, higher resolution  
561           simulations with enough model diversity to explore uncertainty while covering a large enough

562 domain to be useful for many regional interests and are adequate for efforts such as the US  
563 National Climate Assessment and the IPCC.

564 **Acknowledgements**

565 The authors acknowledge Ross Brown and the two anonymous reviewers for their constructive  
566 feedback. This work was supported by the DoE Regional and Global Climate Modeling program  
567 via grants DE-SC0016438 and DE-SC0016605 and the NCAR Regional Climate Uncertainty  
568 Program managed by Dr. Mearns, funded by NSF under the NCAR cooperative agreement. We  
569 acknowledge the WCRP's Working Group on Coupled Modelling and the CMIP5 modeling  
570 groups for producing and making available their model output. We also acknowledge high-  
571 performance computing support provided by NCAR's CISL (Computational and Information  
572 Systems Laboratory 2017), and NCL (The NCAR Command Language 2019). NCAR is  
573 sponsored by the NSF. Livneh data was provided by NOAA/OAR/ESRL PSL. The CRCM5-O  
574 data has been generated and supplied by Ouranos.

575

576

577

578

579

580

581

582

583

584

585 **Declarations**

586 Funding: This work was supported by DoE Regional and Global Climate Modeling grant DE-  
587 SC0016438 and the NCAR Regional Climate Uncertainty Program managed by Dr. Mearns,  
588 funded by NSF under the NCAR cooperative agreement.

589 Conflicts of Interest/Competing Interests: None.

590 Availability of data and material: Snow data from NA-CORDEX will soon be available on  
591 NCAR's Climate Data Gateway (<https://na-cordex.org/data-access.html>) (approximately by  
592 January 2022). Until that point, please reach out to [rmccrary@ucar.edu](mailto:rmccrary@ucar.edu) for data access. CMIP5  
593 Data is available from the WCRP's Earth System Grid Federation Website ([https://esgf-  
594 node.llnl.gov/projects/cmip5/](https://esgf-node.llnl.gov/projects/cmip5/)).

595 Code availability: The code used for this work is available on Rachel McCrary's GitHub  
596 account: ([https://github.com/mccraryclimo/nacordex\\_ClimaticChange\\_Code](https://github.com/mccraryclimo/nacordex_ClimaticChange_Code))  
597 Authors' contributions: McCrary: Writing- Original Draft, Conceptualization, Methodology,  
598 Formal Analysis, Visualization. Mearns: Conceptualization, Supervision, Funding acquisition,  
599 Writing - Review & Editing. Hughes: Writing - Review & Editing. Biner: Investigation (model  
600 simulations), Writing - Review & Editing. Bukovsky: Investigation (model simulations), Writing  
601 - Review & Editing

602

603

604

605

606

607

608 **References**

609 Barnett, T. P., J. C. Adam, and D. P. Lettenmaier (2005) Potential impacts of a warming climate  
610 on water availability in snow-dominated regions. *Nature*, 438:303–309.

611 Barsugli, J. J., et al. (2020). Projections of mountain snowpack loss for wolverine denning  
612 elevations in the Rocky Mountains. *Earth's Future*, 8.

613 Berghuijs, W. R., et al. (2016) Dominant flood generating mechanisms across the United States.  
614 *GRL*, 43:4382– 4390.

615 Brown, R. D., and P. W. Mote (2009) The Response of Northern Hemisphere Snow Cover to a  
616 Changing Climate. *J. Climate*, 22:2124–2145.

617 Brown, R. D. and B. Brasnett (2010) updated annually. Canadian Meteorological Centre (CMC)  
618 Daily Snow Depth Analysis Data, Version 1. Boulder, Colorado USA. NASA National  
619 Snow and Ice Data Center Distributed Active Archive Center.  
620 doi: <https://doi.org/10.5067/W9FOYWH0EQZ3>. Accessed: 15-03-2021.

621 Broxton, P., X. Zeng, and N. Dawson (2019) Daily 4 km Gridded SWE and Snow Depth from  
622 Assimilated In-Situ and Modeled Data over the Conterminous US, Version 1. NASA  
623 NSIDC. Accessed: 19-06-2020.

624 Burakowski, E. and M. Magnusson (2012) Climate Impacts on the Winter Tourism Economy in  
625 the United States. *National Resources Defense Council*, 36 pp.

626 Campbell, C., et al. (2007) Current and Future Snow Avalanche Threats and Mitigation  
627 Measures in Canada. *Canadian Avalanche Center report prepared for Public Safety*  
628 Canada.

629 Campbell, J. L., et al. (2005) Winter in northeastern North America: A critical period for  
630 ecological processes. *Front. Ecol. Environ.*, 3, 314–322.

631 Chin, N., et al. (2018) Assessing potential winter weather response to climate change and  
632 implications for tourism in the US Great Lakes and Midwest. *J. Hydrology: Regional  
633 Studies*, 19:42-56.

634 Christensen, N. S., and Lettenmaier, D. P. (2007). A multimodel ensemble approach to  
635 assessment of climate change impacts on the hydrology and water resources of the  
636 Colorado River Basin. *Hydro Earth Syst. Sci.*, 11(4):1417–1434.

637 Diffenbaugh, N. S., M. Scherer, and M. Ashfaq (2012) Response of snow-dependent hydrologic  
638 extremes to continued global warming. *Nature Climate Change* 3:379–384.

639 ETOPO5 (1988) Data Announcement 88-MGG-02, Digital relief of the Surface of the Earth.  
640 NOAA, National Geophysical Data Center, Boulder, Colorado.

641 Garvert, M. F., , B. Smull, , and C. Mass, 2007: Multiscale mountain waves influencing a major  
642 orographic precipitation event. *J. Atmos. Sci.*, **64**, 711–737.

643 Harpold, A. A. (2016) Diverging sensitivity of soil water stress to changing snowmelt timing in  
644 the Western U.S. *Adv. Water Res.*, 92:16–129.

645 Hughes, M. et al, (2021) Cool season precipitation projections for California and the Western  
646 United States in NA-CORDEX models. *Clim Dynamics*, 56, 3081-3102.

647 Jeong, D. I., and L. Sushama (2018) Projected changes to extreme wind and snow environmental  
648 loads for buildings and infrastructure across Canada. *Sustainable Cities and Society*,  
649 36:225–236.

650 Krasting, J. P., et al., (2013) Future changes in Northern Hemisphere snowfall. *J. Climate*,  
651 26:7813–7828.

652 Livneh B., et al. , 2013: A Long-Term Hydrologically Based Dataset of Land Surface Fluxes and  
653 States for the Conterminous United States: Update and Extensions, *Journal of Climate*,  
654 26, 9384–9392.

655 Luo, Kari, et al., 2020: GlobSnow v3.0 snow water equivalent (SWE). PANGAEA.  
656 <https://doi.org/10.1594/PANGAEA.911944>

657 Lundquist, J., et al. (2020) Our Skill in Modeling Mountain Rain and Snow is Bypassing the  
658 Skill of Our Observational Networks. *BAMS* 100: 2473–2490.

659 Mahoney, K. et al. (2021) Precipitation Projections for California and the Western United States  
660 in NA-CORDEX models. *Climate Dynm.*, 56, 3081-3102.

661 Markhoff, M.S. and A.C. Cullen (2008) Impact of climate change on Pacific Northwest  
662 hydropower. *Climatic Change*, 87:451-469.

663 McCrary, R.R., S. McGinnis, and L.O. Mearns (2017) Evaluation of Snow Water Equivalent in  
664 NARCCAP Simulations, Including Measures of Observational Uncertainty. *J. Hydromet.*,  
665 18:

666 McCrary, R. R., and L. O. Mearns (2019) Quantifying and Diagnosing Sources of Uncertainty in  
667 Midcentury Changes in North American Snowpack from NARCCAP. *J. Hydromet.* 20:  
668 2229–2252.

669 McGinnis, S. and. L. Mearns (2021) Building a climate service for North America based on the  
670 NA-CORDEX data archive. *Climate Services*, 22, 100233.

671 Mearns, L.O., et al. (2015) Uses of Results of Regional Climate Model Experiments for Impacts  
672 and Adaptation Studies: the Example of NARCCAP. *Curr Clim Change Rep*, 1, 1-9.

673 Mearns, L.O., et al. (2017) The NA-CORDEX dataset, version 1.0. NCAR Climate Data  
674 Gateway, Boulder CO, Accessed: 01-06-2020.

675 Mekis, E., et al. (2018) An Overview of Surface-Based Precipitation Observations at  
676 Environment and Climate Change Canada, *Atmosphere-Ocean*, 56:2, 71-95.,

677 Minder, J.R., Letcher, T. W., and Skiles, S. M. (2016) An evaluation of high-resolution regional  
678 climate model simulations of snow cover and albedo over the Rocky Mountains, with  
679 implications for the simulated snow-albedo feedback, *J. Geophys. Res. Atmos.* 121:  
680 9069– 9088.

681 Mudryk, L., et al. (2020) Historical Northern Hemisphere snow cover trends and projected  
682 changes in the CMIP6 multi-model ensemble. *The Cryosphere* 14:2495-2514.

683 Muñoz-Sabater, J., (2019): ERA5-Land hourly data from 1981 to present. Copernicus Climate  
684 Change Service (C3S) Climate Data Store (CDS). Accessed:10-06-2020),  
685 10.24381/cds.e2161bac

686 Musselman et al. (2015) Impact of windflow calculations on simulations of alpine snow  
687 accumulation, redistribution and ablation, *Hydro. Processes*, 29(18) 3983-3999.

688 Musselman et al, (2017) Slower snowmelt in a warmer world. *Nature Climate Change*. 7, 214-  
689 219.

690 NOHRSC, 2004: *Snow Data Assimilation System (SNODAS) Data Products at NSIDC, Version*  
691 *1*. NSIDC. Accessed: 12-06-2019.

692 Notaro, M., et al. (2014) Twenty-first-century projections of snowfall and winter severity across  
693 central-eastern North America. *J. Climate* 27:6526–6550.

694 Notaro, M., et al. (2015) Dynamically Downscaled Projections of Lake-Effect Snow in the Great  
695 Lakes Basin. *J. Climate* 28: 1661-1684.

696 Palko, K. and Lemmen, D.S. (Eds.). (2017). Climate risks and adaptation practices for the  
697 Canadian transportation sector 2016. Ottawa, ON: Government of Canada.

698 Qin, Y et al. (2020) Agricultural risks from changing snowmelt. *Nat. Clim. Chang.* 10:459–465.

699 Räisänen, J. (2008) Warmer climate: less or more snow? *Climate Dynamics*, 30: 307–319.

700 Rasmussen, R., et al. (2011) High-Resolution Coupled Climate Runoff Simulations of Seasonal  
701 Snowfall over Colorado: A Process Study of Current and Warmer Climate. *J.Climate*  
702 24:3015–3048.

703 Rhoades, A. M., A. D. Jones, and P. A. Ullrich, 2018a: The Changing Character of the California  
704 Sierra Nevada as a Natural Reservoir. *GRL*, 45, 13,008-13,019.

705 Rhoades, A. M., P. A. Ullrich, and C. M. Zarzycki, 2018b: Projecting 21st century snowpack  
706 trends in western USA mountains using variable-resolution CESM. *Clim Dyn*, 50, 261–  
707 288.

708 Sun et al. (2018) Understanding End-of-Century Snowpack Changes over California’s Sierra  
709 Nevada. *GRL*. 46(2). 933-943.

710 Taylor, K. E., R. J. Stouffer, and G. A. Meehl (2012) An Overview of CMIP5 and the  
711 Experiment Design. *BAMS* 93:485–498.

712 U.S. National Ice Center. 2008, updated daily. IMS Daily Northern Hemisphere Snow and Ice  
713 Analysis at 1 km, 4 km, and 24 km Resolutions, Version 1. [1997-2010]. Boulder,  
714 Colorado USA. NSIDC: National Snow and Ice Data Center.  
715 doi: <https://doi.org/10.7265/N52R3PMC>.

716 Vavrus, S. (2007) The role of terrestrial snow cover in the climate system. *Climate Dynamics*,  
717 29: 73–88.

718 Walton, D et al. (2021) Understanding Differences in California Climate Change Projections  
719 Produced by Dynamical and Statistical Downscaling. *JGR Atmo.*, 125(10).

720 Westerling, A. L. et al. (2006) Warming and Earlier Spring Increase Western U.S. Forest  
721 Wildfire Activity. *Science*, 313:940–943.

722 Wobus, C. et al., (2017) Projected climate change impacts on skiing and snowmobiling: A case  
723 study of the United States. *Global Environmental Change*, 45:1-14,  
724 doi:10.1016/j.gloenvcha.2017.04.006.q

725 Xia, Y., et al., NCEP/EMC (2012), NLDAS Noah Land Surface Model L4 Hourly 0.125 x 0.125  
726 degree V002, Edited by David Mocko, NASA/GSFC/HSL, GES DISC, Accessed: [10-  
727 06-2019], [10.5067/47Z13FNQODKV](https://doi.org/10.5067/47Z13FNQODKV)

728

729

730

731

732

733

734

735

736

737

738

739

740

741

742

743 **Tables**

744 **Table 1.** The NA-CORDEX RCMs and their driving CMIP5 GCMs examined in this  
 745 study. Each column displays the resolution (0.44° or 50km; 0.22° or 25km) of the RCM  
 746 simulations or the resolution of the driving GCM. Snow is not available from the EC-EARTH  
 747 GCM simulation, but is available from the HIRHAM5 RCM driven with EC-EARTH boundary  
 748 conditions.

749

GCM/RCM	CanRCM4	CRCM5-U	CRCM5-O	WRF	HIRHAM5	GCM Resolution
<b>HadGEM2-ES</b>	-	-	-	50km/25km	-	1.25 x 1.875°
<b>CanESM2</b>	0.44°/0.22°	0.44°/0.22°	-/0.22°	-	-	~2.8° x ~2.8°
<b>CNRM-CM5</b>	-	-	-/0.22°	-	-	~1.4°x ~1.4°
<b>MPI-ESM-LR</b>	-	0.44°/0.22°	-/0.22°	50km/25km	-	~1.87° x ~1.87
<b>MPI-ESM-MR</b>	-	0.44°/0.22°	-	-	-	~1.87° x ~1.87
<b>EC-EARTH</b>	-	-		-	0.44°/-	-
<b>GFDL-ESM2M</b>	-	-	-/0.22°	50km/25km	-	~2.0° x 2.5°

750

751

752

753

754

755

756 **Table 2.** Table of model-informed observational datasets (MObs) used in this study.

Product	Resolution	Domain	Frequency	Time Period	Reference
SNODAS	1km	CONUS	Daily	2003-2020	NOHRSC (2004)
UA-SWE	4km	CONUS	Daily	1981-2020	Broxton et al. (2019)
Livneh	0.0625° (~6km)	CONUS	Daily	1950-2013	Livneh et al. (2015)
ERA5- land	0.1° (~9km)	Global	Hourly	1981-2020	Munoz-Sabater (2019)
NLDAS- noah	0.125° (~13km)	CONUS	3-hourly	1979-2020	Xia et al. (2012)
NLDAS- vic	0.125° (~13km)	CONUS	3-hourly	1979-2020	Xia et al. (2012)
GlobSnow v.3	25km	N. Hemisphere	Daily	1979-2020	Luoju et al. (2020)
CMC	24km	N. America	Monthly	1998-2020	Brown and Brasnett (2010)

757

758

759

760

761

762

763

764

765

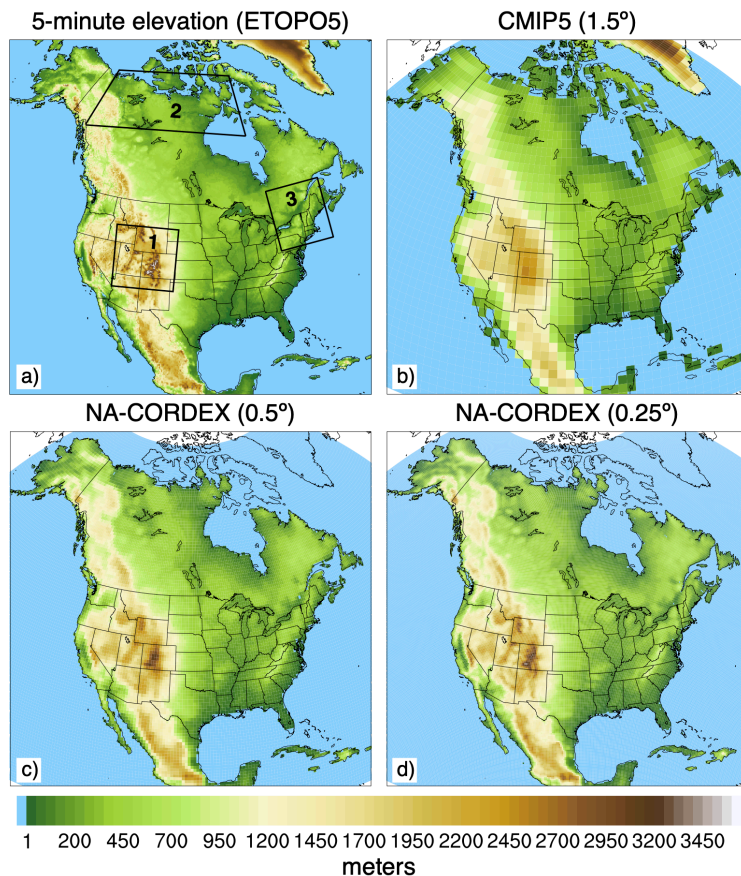
766

767

768

769 **Figures**

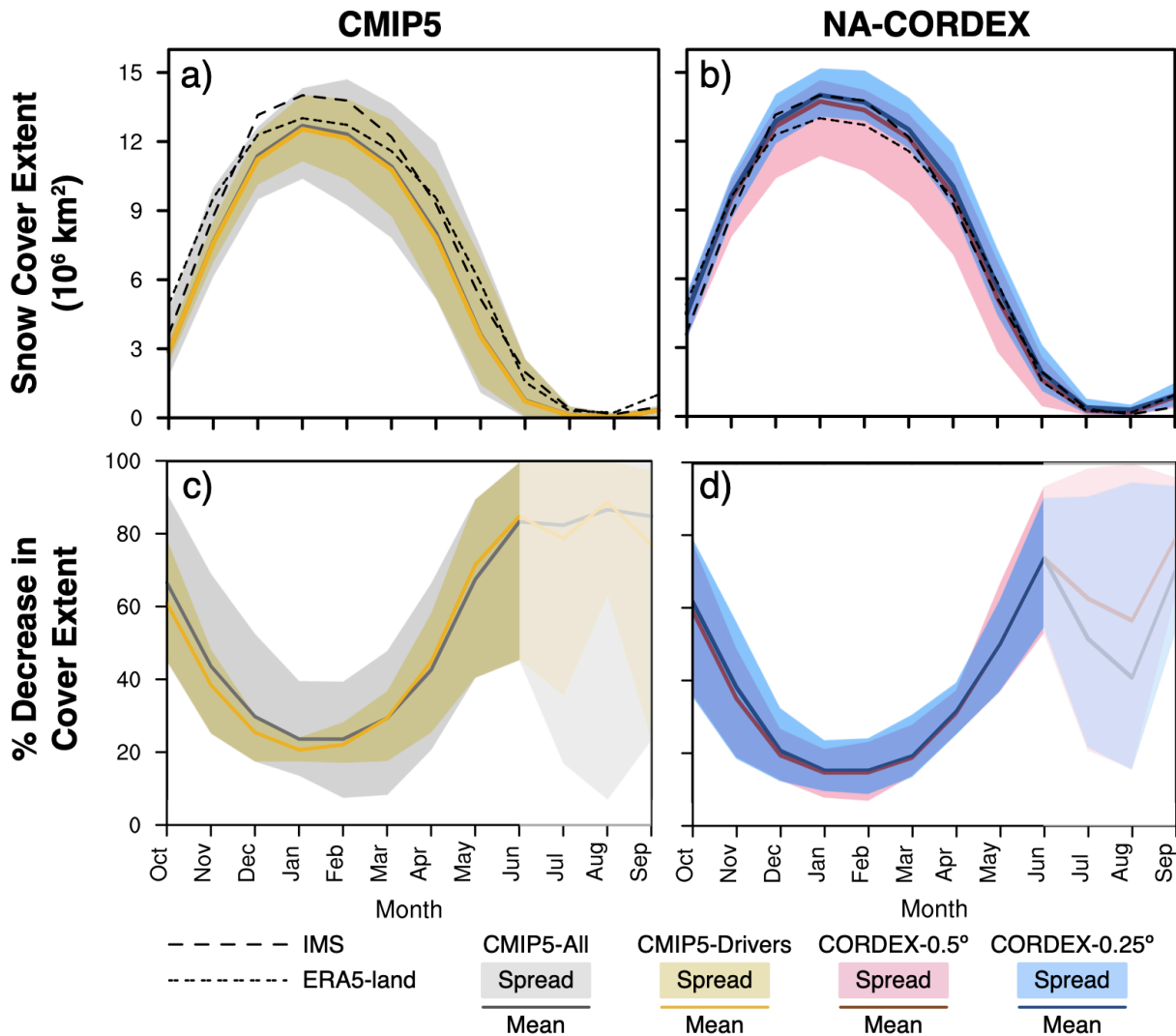
770  
771  
772



773  
774  
775 **Fig. 1** Representation of topography from the 5-minute ETOPO5 (1988) dataset (a), the  
776 ensemble-average topography from the CMIP5-Driver ensemble (b), the NA-CORDEX-0.5°  
777 ensemble (c) and the NA-CORDEX (0.25°) ensemble. The three sub-regions examined are  
778 outlined in (a) where (1) is the U.S. Intermountain West, (2) is North-Central Canada, and (3) is  
779 the Northeast U.S. and Southeast Canada.

780  
781  
782  
783  
784  
785  
786  
787  
788  
789

790  
791  
792



793  
794 **Fig. 2** The annual cycle of monthly mean NA SCE from the MObs (dashed lines on a and b) and  
795 the historical climate simulations from the two CMIP5 ensembles (a) and two NA-CORDEX  
796 ensembles (b) examined in this study. Also shown is the annual cycle of the percent decrease in  
797 NA SCE projected for the end-of-century from the CMIP5 ensembles (c) and the NA-CORDEX  
798 ensembles (d). The spread of each ensemble is displayed with colored shading. The average of  
799 each ensemble is plotted with a corresponding solid line. Percent decreases in SCE for July-  
800 September have been masked as they are skewed by small number division. NA SCE has been  
801 calculated using the native grid of all models and datasets.

802  
803  
804  
805  
806

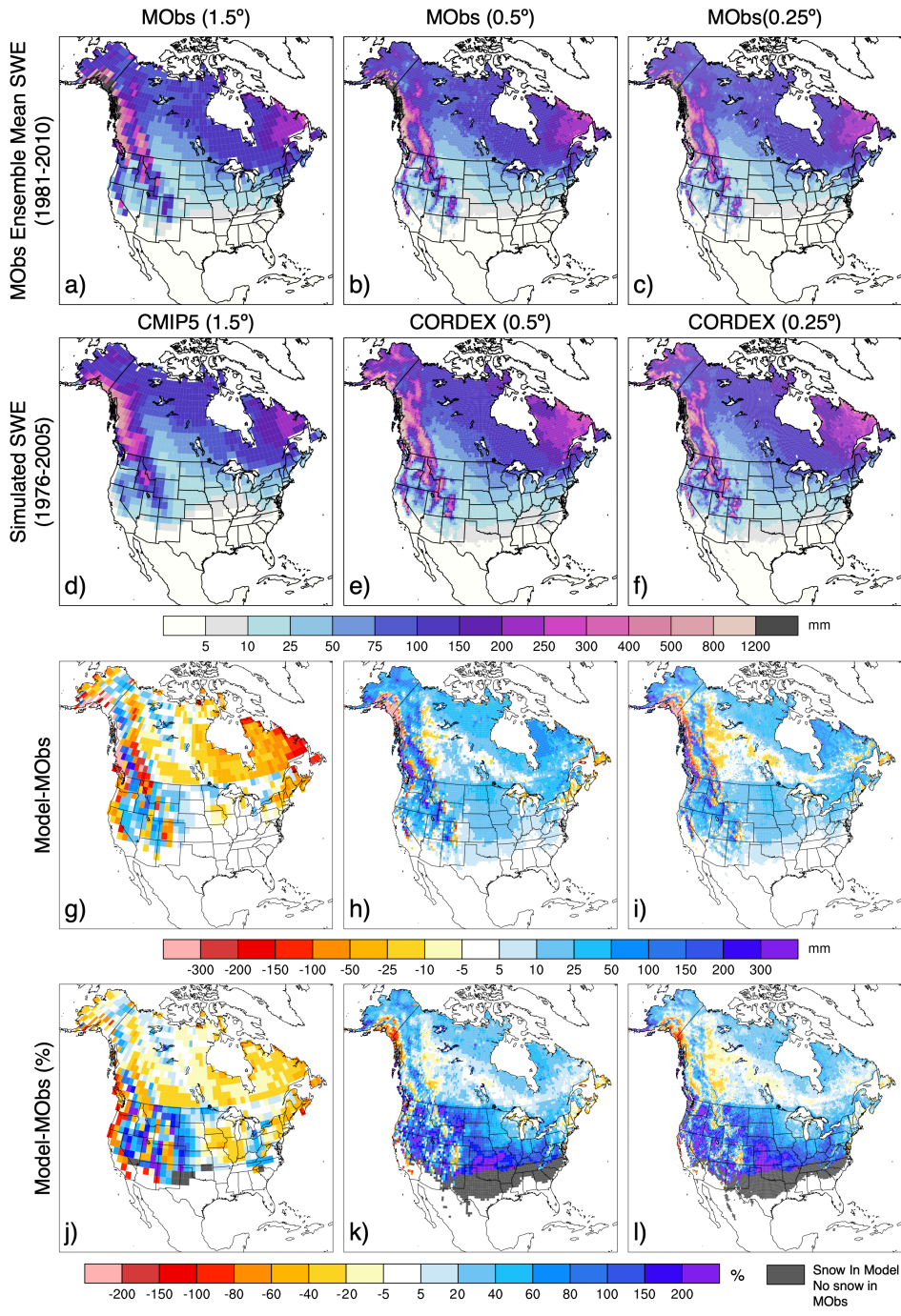
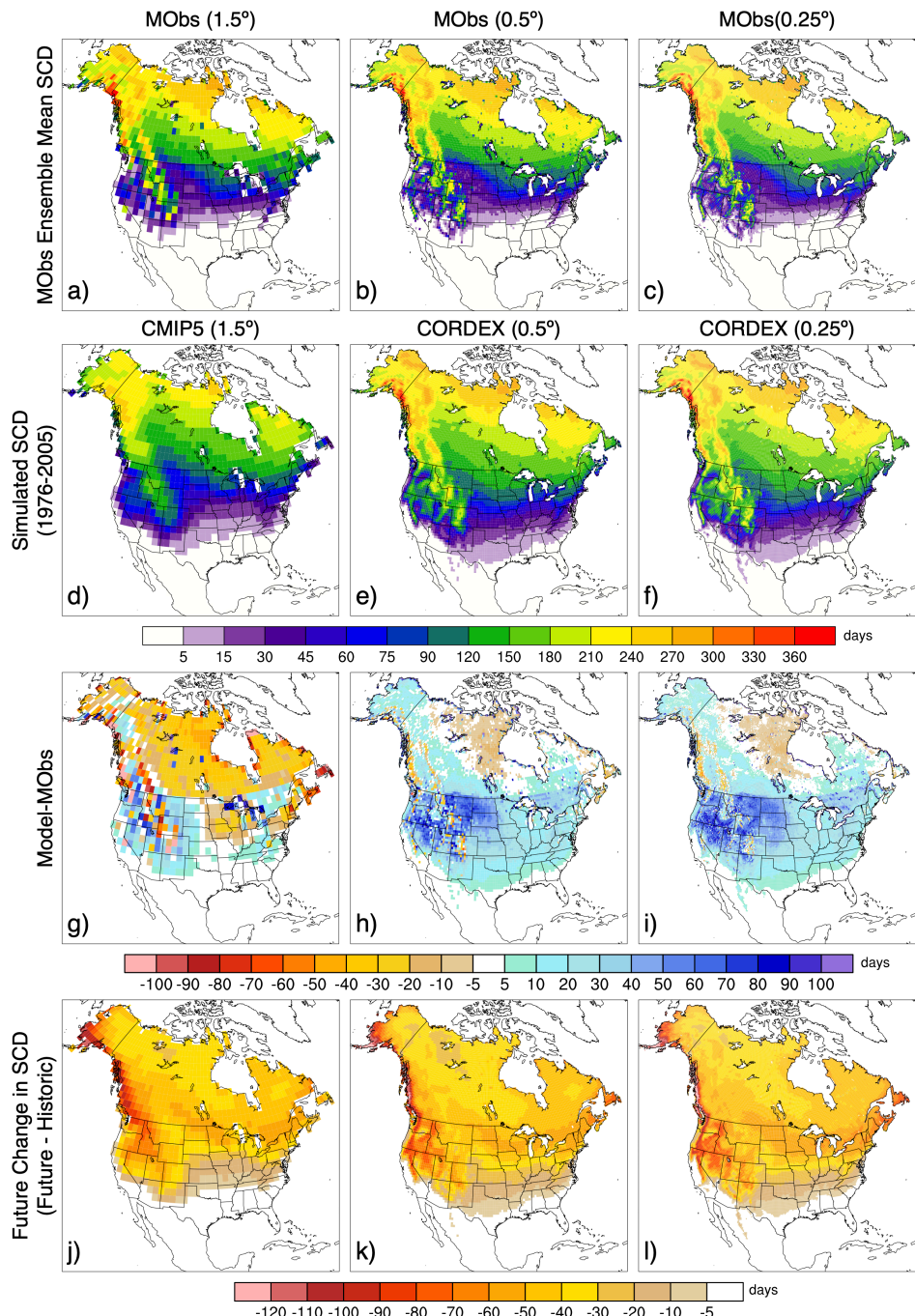
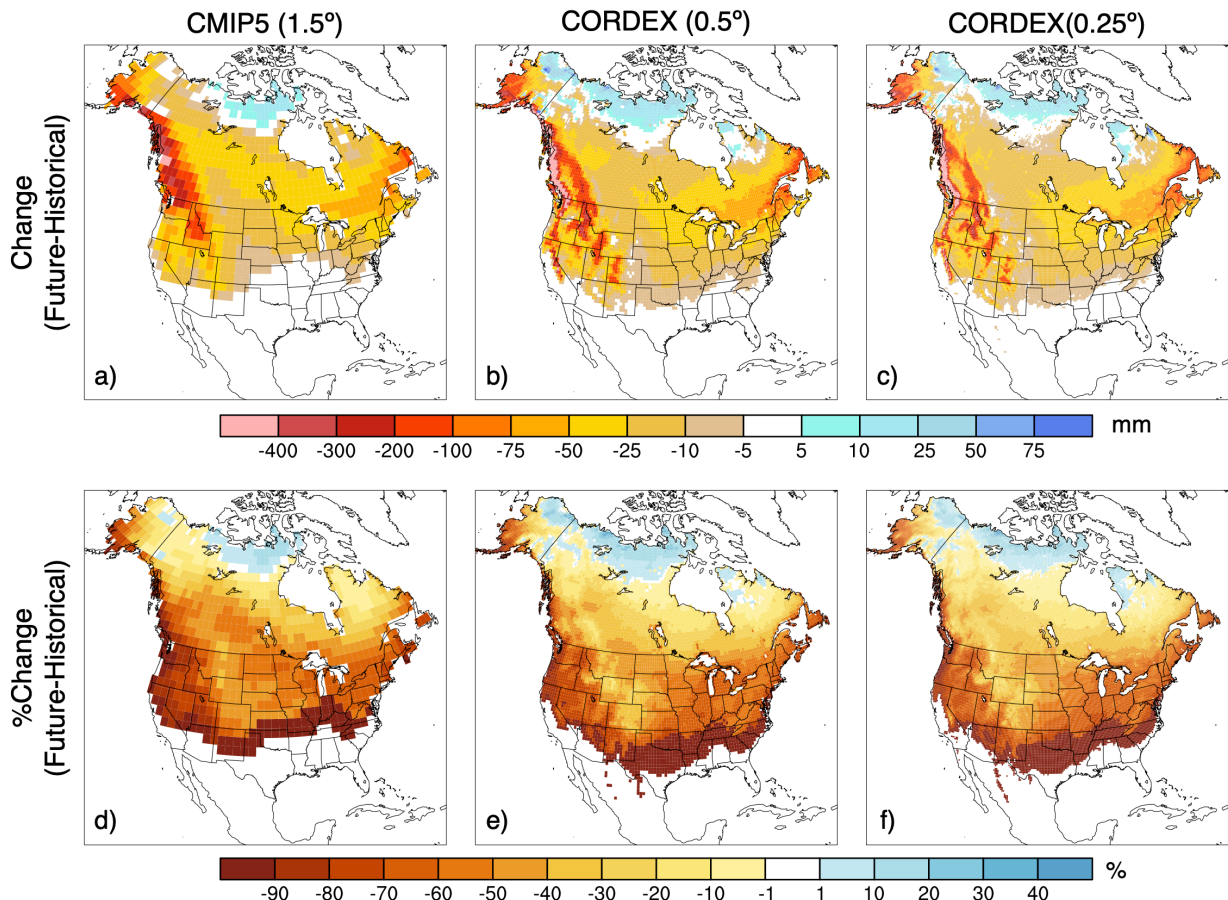


**Fig. 3** Maps of the average annual monthly maximum SWE (AM-SWE) from the MObs ensemble mean which has been regridded to the common  $1.5^\circ$ ,  $0.5^\circ$  and  $0.25^\circ$  resolution (a-c). Ensemble mean AM-SWE from the historical time period for the three model ensembles (d-f). Also shown are the magnitude (g-i) and percent (j-l) of the simulated bias (model – MObs) of AM-SWE. The MObs ensemble mean is calculated independently at each gridbox using datasets with available data (See SI Figs. S9-S11).

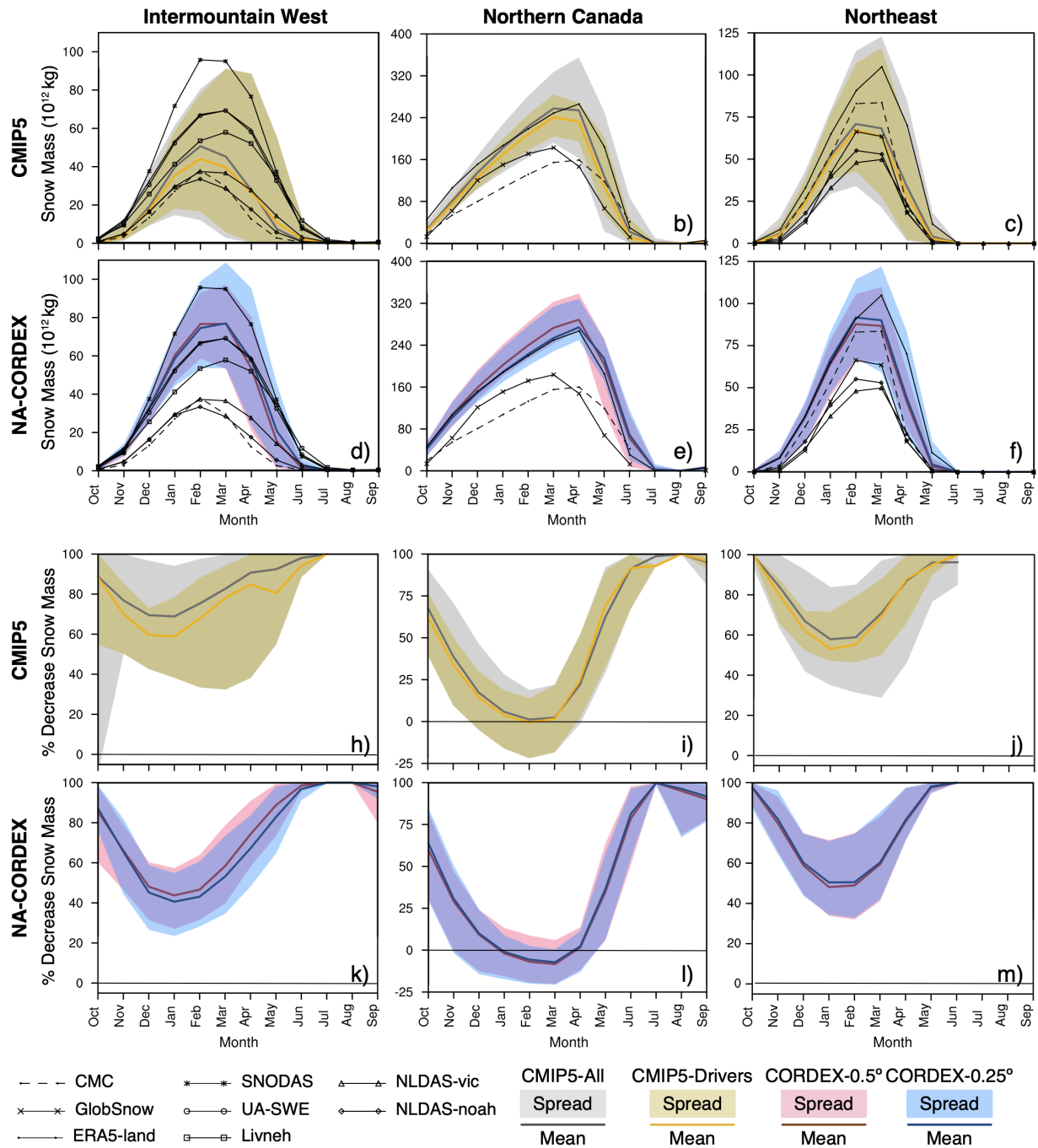


819 **Fig. 4** Maps of snow cover duration (SCD) from the MObs ensemble mean regressed to the  
 820 common  $1.5^\circ$ ,  $0.5^\circ$  and  $0.25^\circ$  grids (a-c), and the ensemble mean SCD from the historical time  
 821 period from each model ensemble (d-f). Also shown are the simulated bias in SCD (model-  
 822 MObs, g-i) and the future change in SCD (future-historical, j-l). The MObs ensemble mean is  
 823 calculated independently at each gridbox using datasets with available data (See SI Figs. S21-  
 824 S23).

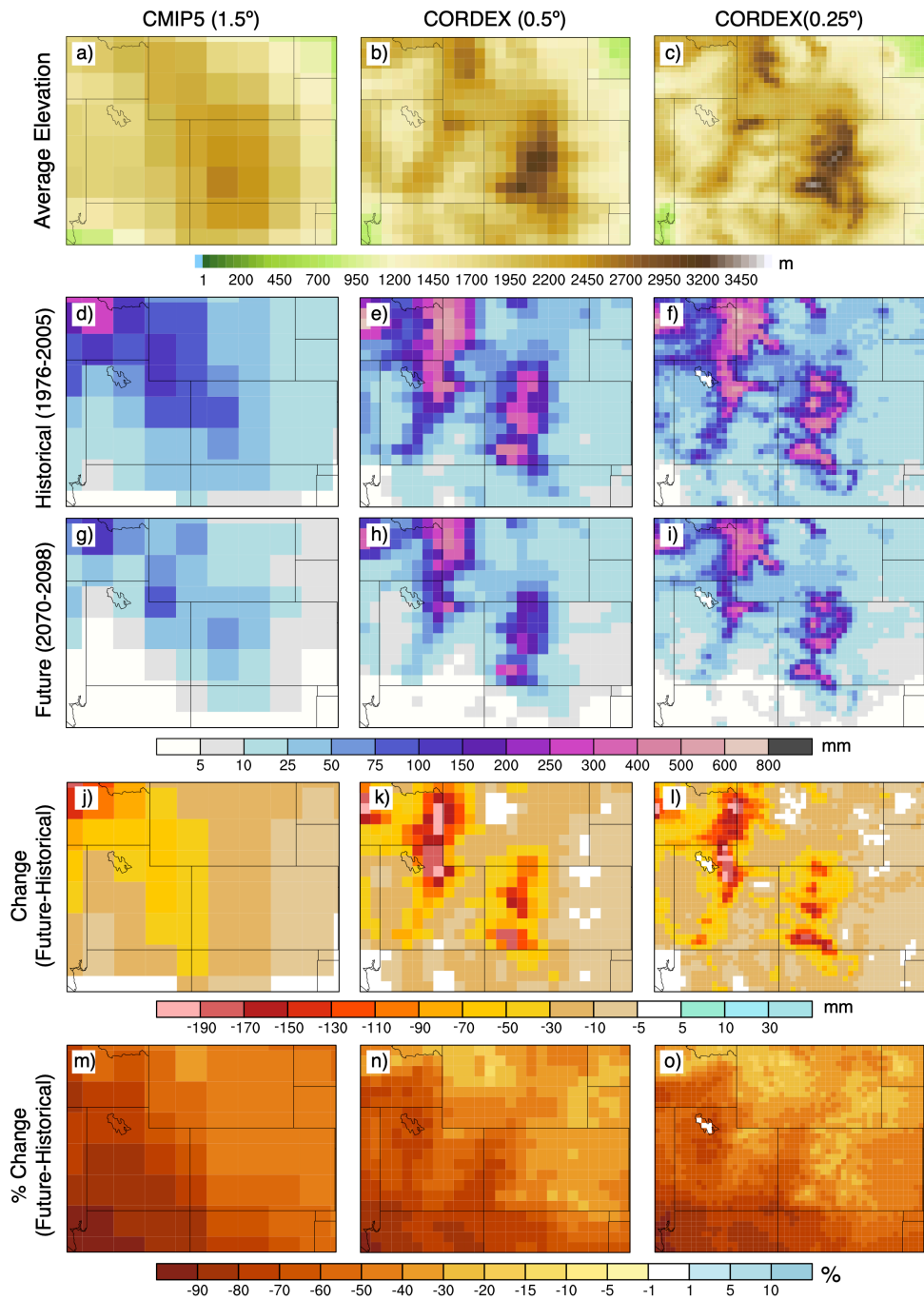
827  
828  
829  
830



831  
832  
833 **Fig. 5** Maps of the magnitude (a-c) and percent (d-f) change in ensemble mean AM-SWE  
834 projected by the end-of-the century by the three model ensembles (Future-Historic).  
835  
836  
837  
838  
839  
840  
841  
842  
843  
844  
845  
846  
847  
848  
849

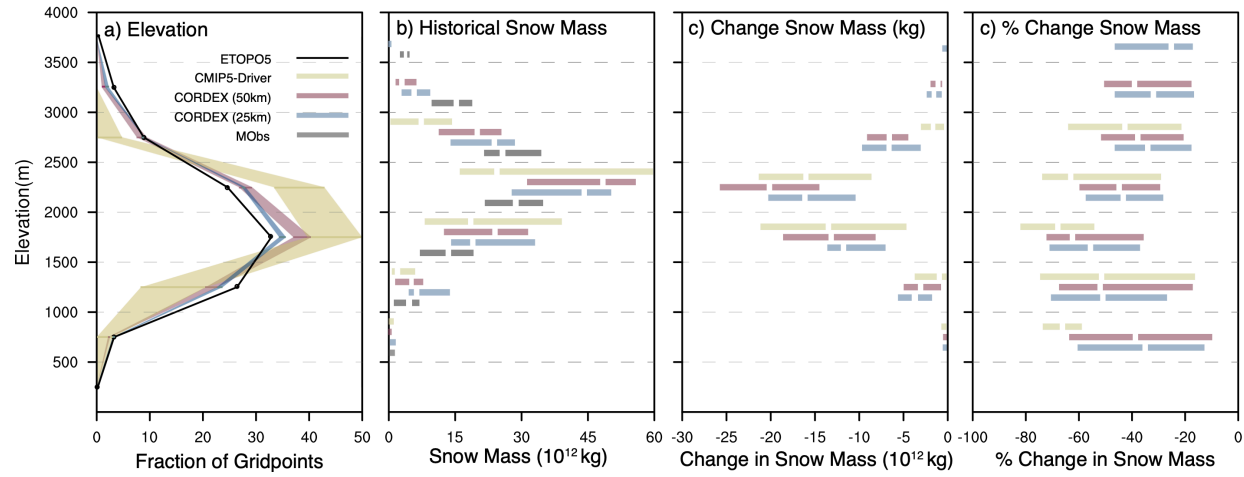
850  
851852  
853  
854  
855  
856  
857  
858

**Fig. 6** The first two rows show the annual cycle of SM from the CMIP5-All and CMIP5-Driver ensembles (a-c), the NA-CORDEX ensembles (d-f) and available MObs, for the IMW (a,d), NC-Canada (b,e), and Northeast (c,f) regions. The last two rows show the percent decrease SM projected for the end of the century for the CMIP5 (h-j) and NA-CORDEX ensembles (k-m). All regional averages are calculated on each model's native grid.



859  
860 **Fig. 7** Maps over the IMW region of the ensemble mean topography (a-c), ensemble mean  
861 historic AM-SWE (d-f), ensemble mean future AM-SWE (g-i), and the magnitude (j-l) and  
862 percent change (Future-Historic) in AM-SWE from the three model ensembles.  
863  
864  
865  
866  
867  
868

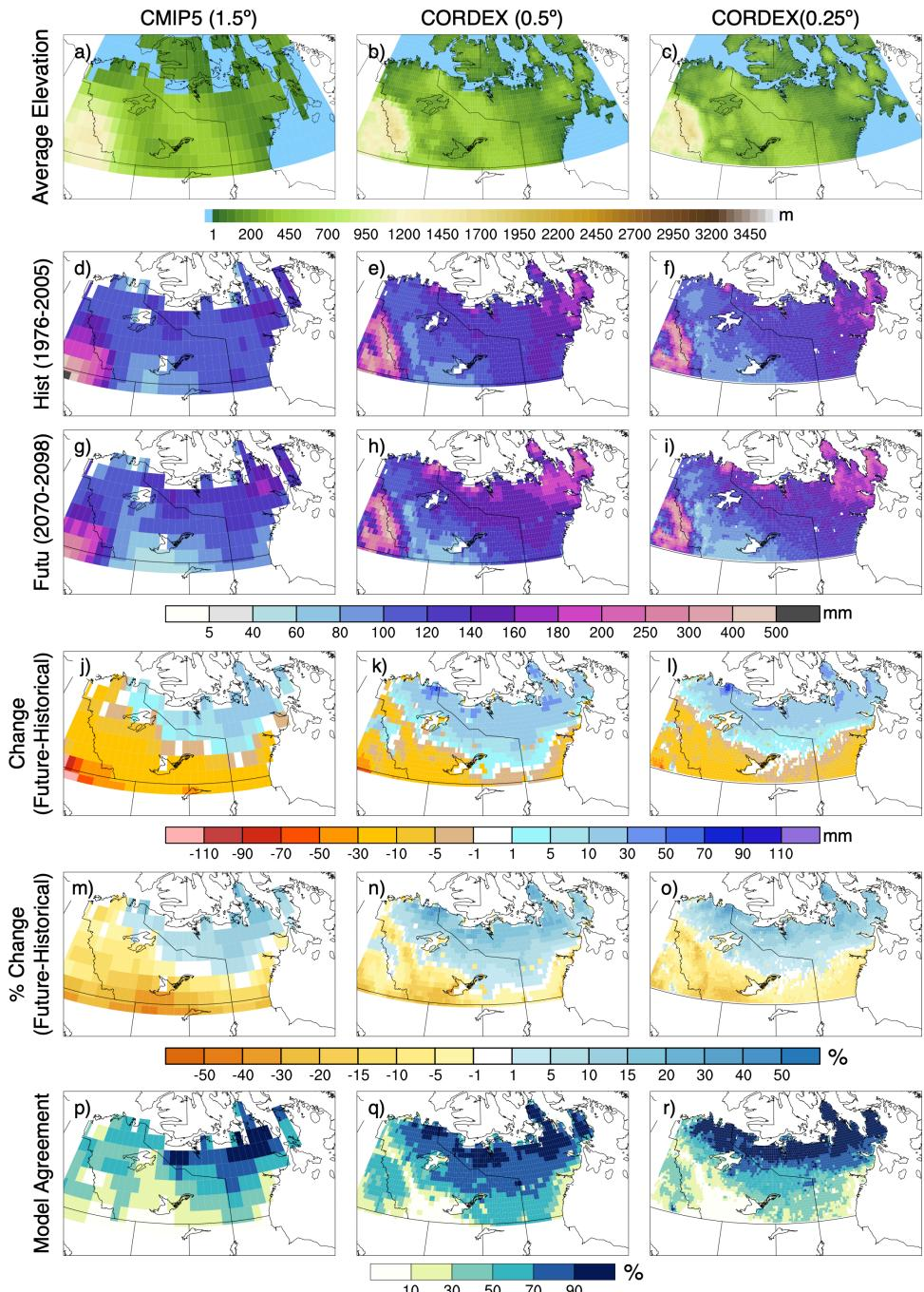
869  
870  
871  
872  
873  
874



875  
876  
877  
878  
879  
880  
881  
882  
883  
884  
885

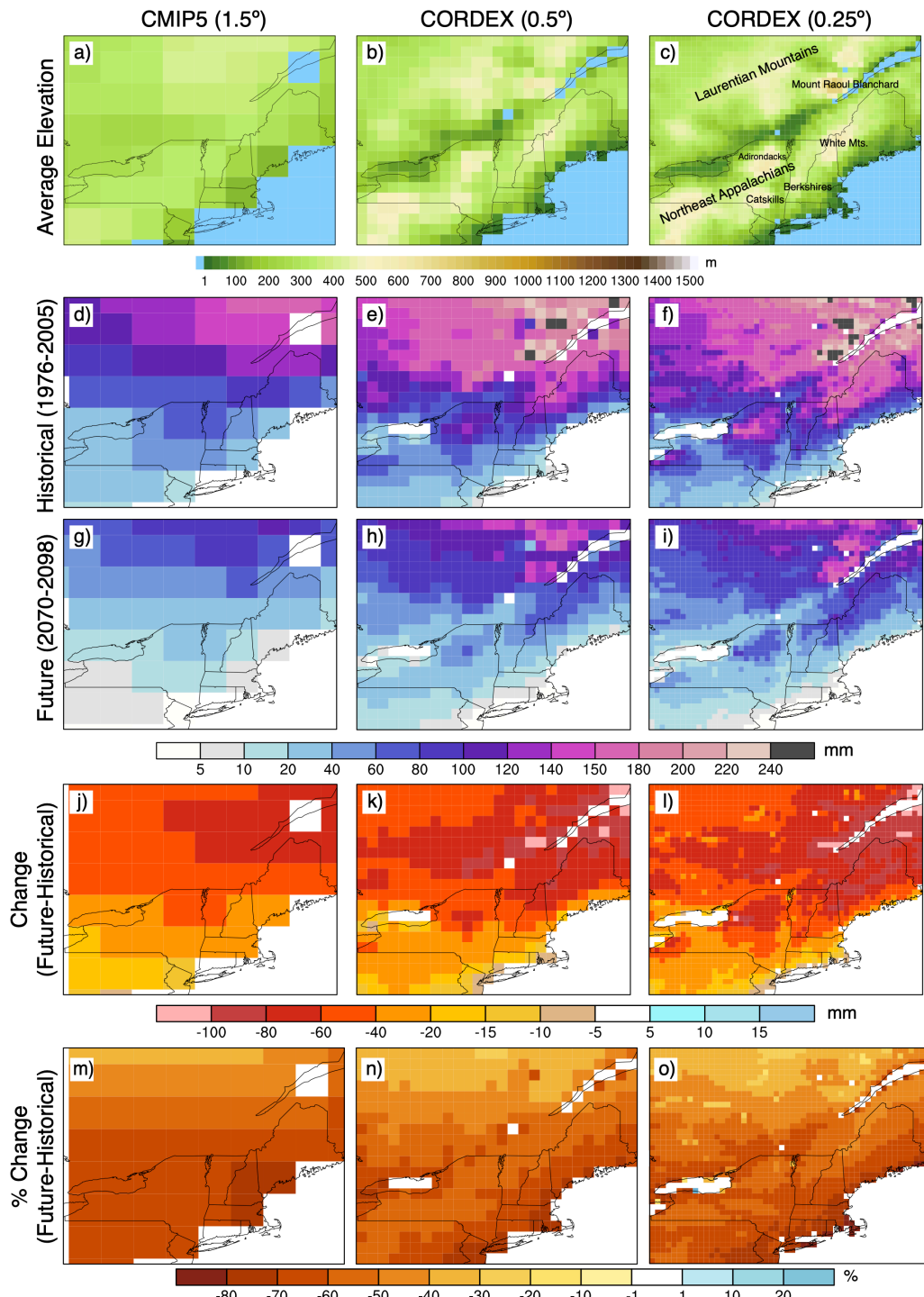
**Fig. 8** The distribution of elevation for the IMW region from ETOPO5, and the three different model ensembles (a). The elevational distribution of historical AM-SM from the four MObs with the highest peak SM and the three model ensembles (b), the magnitude in future change in AM-SM (c), and the percent change in AM-SM (c). Elevation bins range from 0-4000m, incremented by 500m. Values are plotted between the elevation bins identified by the dashed lines. In (a) elevation is binned independently for each model using its native grid topography. The spread for each ensemble shows the minimum and maximum values calculated for each bin. In b-d the spread of each ensemble is shown, and the white space between the bars represents the ensemble mean change.

886  
887  
888  
889  
890  
891  
892  
893  
894  
895



896  
897  
898  
899  
900  
901  
902  
903  
904

**Fig. 9** Maps over the NC-Canada region of the ensemble mean topography (a-c), ensemble mean historic AM-SWE (d-f), ensemble mean future AM-SWE (g-i), the magnitude (j-l) and percent (m-o) change (Future-Historic) in AM-SWE, and the percent of models in each ensemble that agree AM-SWE will increase in the future (p-r).



905  
906 **Fig. 10** Maps over the Northeast region of ensemble mean topography (a-c), ensemble mean  
907 historic AM-SWE (d-f), ensemble mean future AM-SWE (g-i), the magnitude (j-l) and percent  
908 (Future-Historic) in AM-SWE from the three model ensembles.  
909  
910